COMPUTATIONAL FLUID DYNAMICS ANALYSIS OF NEW CONCEPT HEAT EXCHANGER FOR OTEC APPLICATION

Muhammad Farhan Azwan Mohd Farid[a], Chiong Meng Soon[b*], Mahadhir Mohammad[b], Chun Mein Soon[b]

[a]Faculty of Mechanical Engineering, Universiti Teknologi Malaysia, 81310 UTM Johor Bahru, Johor, Malaysia
[b]UTM LoCARtic, Institute for Sustainable Transport (IST), Universiti Teknologi Malaysia, 81310 UTM Johor Bahru, Johor, Malaysia

Article history
Received
7th November 2024
Received in revised form
8th December 2024
Accepted
8th December 2024
Published
26th December 2024

*Corresponding author
chiongms@utm.my

GRAPHICAL ABSTRACT

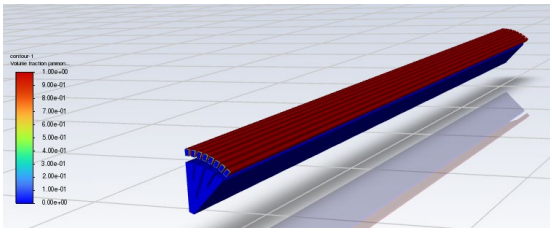

ABSTRACT

This paper presents a comprehensive analysis of a new concept of heat exchanger for Ocean Thermal Energy Conversion (OTEC) applications. The study utilizes Computational Fluid Dynamics (CFD) simulations to evaluate the performance of different heat exchanger designs for extracting thermal energy from oceanic sources, specifically using water and R717 liquid. Key performance parameters including cold vapor fraction, temperature difference, and pressure drop are evaluated through a combination of numerical simulations and experimental validations. The analysis of the cold vapor fraction provides insights into evaporation rates and their distribution across multiple prototypes, highlighting the impact of the wetted area on heat transfer effectiveness. The evaluation of temperature differences reveals variations in discharge fluid temperatures, with some prototypes deviating from thermodynamic principles at a default evaporation frequency of 0.1. Various evaporation frequencies are simulated and compared with experimental data to select the optimal frequency for each prototype. The simulations and experiments, conducted under similar conditions, ensure accurate validation despite inconsistencies arising from variations in heat exchanger design and boundary conditions. The performance evaluation demonstrates the effectiveness of the three prototypes, with Prototype 2 achieving the highest effectiveness up to 59% for OTEC applications. The findings contribute to a better understanding of heat exchanger performance in OTEC and provide valuable insights for design optimization and future application development. This paper emphasizes the significance of efficient heat transfer and highlights the potential of ocean thermal energy as a renewable and sustainable resource.

KEYWORDS

OTEC, Heat exchanger, Evaporation frequency, ANSYS simulation, Effectiveness

INTRODUCTION

Renewable energy, which is characterized by its ability to reduce costs and provide a future with pure energy, has experienced remarkable growth. Renewable energy has the potential to substantially reduce carbon emissions and other forms of pollution by substituting fossil fuels in the power sector[1], [2]. Ocean Thermal Energy Conversion (OTEC), which utilizes temperature differences between the surface and depths of the ocean to generate electricity, is one of the developing technologies in renewable energy generation [3].

OTEC facilities utilize a closed Rankine cycle, which consists of pumps, turbine generators, and heat exchangers including the evaporator and condenser. Warm surface water is circulated

through the evaporator in this process, transforming a working fluid into a vaporized fluid that operates the turbine. The condenser, which is chilled by cold ocean water from greater depths, returns the vaporized fluid to its liquid state. However, due to the independent evaluations of heat transfer coefficient and pressure drop, selecting an appropriate and highly efficient heat exchanger design for OTEC applications remains challenging [4][5]. Figure 1 shows the classification of HEX based on their construction.

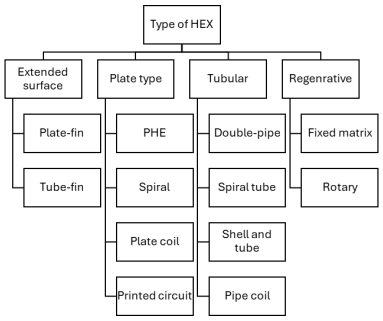

Figure 1: Classification of HEXs based on their construction [6].

As an essential component of the heat exchanger, the evaporator facilitates the conversion of liquid to gas phase. It uses the temperature distribution of cold surface seawater within the closed system to generate saturated vapor from the working fluid. The success of the Rankine cycle is determined by the expansion of the vapor through the turbine, which recovers more energy than is required to pressurize the liquid once more [7]. Consequently, the effectiveness of the evaporator in converting R717 liquid to vapor, especially in terms of its volume fraction, has a significant impact on energy conversion efficiency. During the evaporation process, heat transfer processes occur between the evaporator's walls. Several parameters, including wetted area, temperature difference, overall heat transfer coefficient, and wall thickness, are variable in this study, whereas the thermal conductivity and emissivity coefficient are constants [8].

To evaluate the effectiveness of the new concept evaporator design, parameters such as temperature, pressure, and vapor fraction must be measured and computed using specialized heat transfer simulation software such as Ansys Fluent. Ansys Fluent is a versatile computational fluid dynamics (CFD) application that can simulate fluid flow, heat, and mass transfer. Through CFD, this study aims to investigate the effectiveness performance of the new evaporator concept for OTEC application. This research utilized the working fluid of water as the hot fluid and R717 (ammonia) liquid as the cold fluid which ammonia proves a significant outcome for a closed Rankine Cycle. The R717 vapor formed along the evaporator will be discussed based on the findings of the research [9].

METHODOLOGY

The method that will be used to evaluate the performance of the evaporator is Computational Fluid Dynamics (CFD) by using Ansys Fluent where three prototypes were simulated for multiphase simulation. It is the technique of solving partial differential equations, particularly the continuity equation and the momentum or Navier-Stokes equations. The simulation will involve the heat transfer between two different fluids which are R717 liquid and water based on the boundary condition that has been decided involving mass flow rate, inlet temperature as well as outlet pressure. Table 1 shows the boundary condition for the simulation of the prototype. Figure 2 shows the Flowchart of the simulation in ANSYS Fluent.

Table 1: Boundary condition of the prototype.

Boundary Condition	Unit	Water	R717 liquid
Mass flow rate, $\dot{m}$	kg/s	1.5	0.0116
Inlet Temperature, T_{in}	K	303.15	287.45
Outlet Pressure, P_{out}	Pa	101325	958000

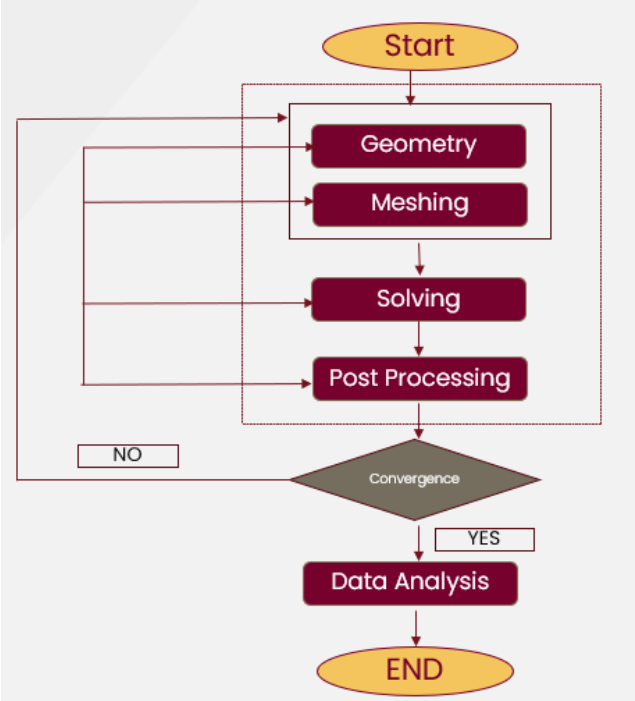

Figure 2: Flowchart of the simulation in ANSYS Fluent

Prototype Dimension

Three prototypes are designed and modelled by using SOLIDWORKS which the prototype was designed as part of a cross-section from a whole circle of the evaporator. Prototype 1 has a cross section of 45° while Prototypes 2 and 3 are 15° (refer Figure 3). This is to reduce the computational time for the multiphase simulation. Table 2 shows the dimensions of each prototype. Lengths for each prototype are the same but the difference is wall thickness for hot fluid.

Table 2: Dimension of each prototype

Prototype	Wall Thickness (mm)	Evaporator Length (mm)
Prototype 1	2.75	500
Prototype 2	0.5	500
Prototype 3	0.5	500

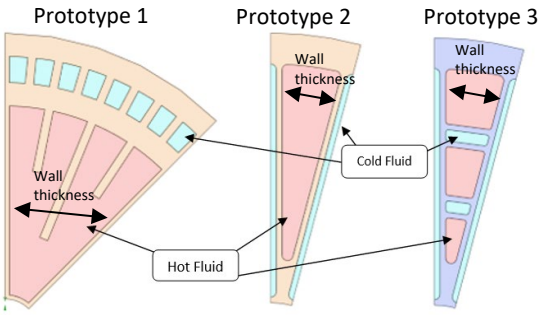

Figure 3: Design of Prototypes 1, 2, and 3.

Mesh Generation

CFD meshing, similarly meshing in finite element simulations, applies a numerical grid to a fluid body and boundary. The precision of a CFD simulation is determined by groupings of grid points produced by meshing methods. The meshing system's physics preference is set to CFD, and the solver preference is set to Fluent. Fixed at 0.001m, the element size of the models provides a finer and more compact geometry. The initial mesh method is generated by applying body sizing to all body interfaces with a 0.001m element size. When the boundary condition analysis is performed correctly by creating a finer mesh near the wall or boundary, the inflation method is then applied to all bodies involved in fluid fluxes as it is a fundamental technique. The selected inflation option is first layer thickness with a first layer height of 0.0001m and a maximum of 3 layers. All these parameters are shown in Table 3.

Table 3: Element size of the meshing parameters

Meshing Type	Element size (m)
Body Sizing	0.001
Inflation	0.0002

Each prototype has an individual number of nodes and elements, with a higher number of nodes and elements requiring more computational time due to their complexity but providing more precise results [10]. Table 4 depicts the number of nodes and elements for each prototype.

Table 4: Number of nodes and elements for each prototype.

Prototype	Nodes	Elements
Prototype 1	669444	544245
Prototype 2	582950	459170
Prototype 3	358082	284993

Mesh Quality

Mesh quality in ANSYS refers to how well the mesh matches the models' geometry. It is essential for a high-quality to have well-shaped and uniformly sized parts. This is essential for the simulation's accuracy and dependability. Orthogonal quality and skewness are the main criteria that can be used to evaluate the quality of the mesh in ANSYS.

Table 5: Mesh quality for all prototypes.

Prototype	Minimum Orthogonal Quality	Maximum Skewness
Prototype 1	0.45883	0.69929
Prototype 2	0.32132	0.7796
Prototype 3	0.073033	0.92697

As the minimum orthogonal quality is greater than 0.01 and the maximum skewness is less than 0.95, both parameters indicate a mesh of high quality [11]. When simulating the model in ANSYS Fluent, a higher mesh accuracy will result in a more accurate simulation.

Solver Setup

Setting up a simulation with Fluent requires defining the geometry of the problem, configuring the fluid properties and boundary conditions, and selecting the appropriate solver and numerical options. This initialization procedure determines the dependability and utility of simulation results. Before performing the calculation for all prototypes, the initial setup includes the parameters for general, models, materials, boundary conditions, and methods. Table 6 shows the solver setup settings used throughout the

simulations. Figure 4 shows the solver setup simulation.

Table 6: Solver setup for multiphase simulation

Setup	Choice
Solver	Pressure Based
Time	Transient
Multiphase Model	Volume of Fluid (VOF)
Turbulence Model	k-epsilon
Boundary Conditions	Mass flow inlet Pressure outlet

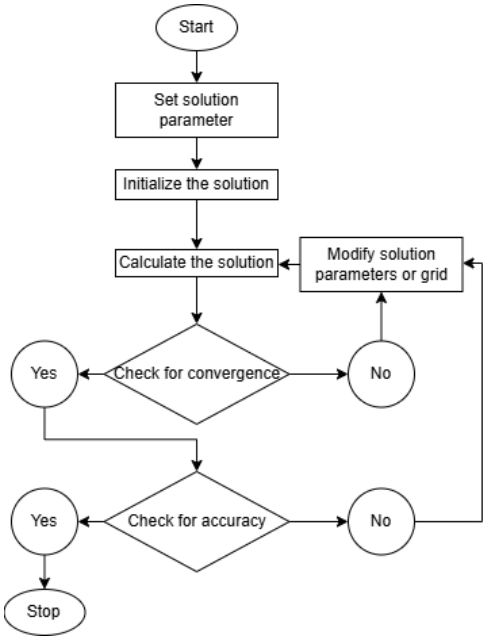

Figure 4: Flowchart of the solver setup simulation

Solver Setup

Standard initialization is applied in this instance because the model must be modified to account for the water volume fraction in the interior fluid part. Since the multiphase model only specifies one principal phase throughout the model, there will be two phases which are water and R717 liquid, in the evaporator pipe. Before conducting the simulation, R717 vapor needs to be patched into inner the fluid section to initiate the system to account for the formation of R717 vapor after the simulation. Figure 5 shows the patching method for R717 vapor.

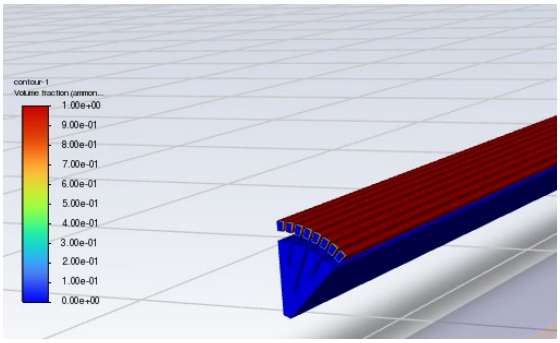

Figure 5: Patching methods for R717 vapor.

Evaporation Frequencies

The frequency of phase change of evaporation should be considered while modeling multiphase in ANSYS Fluent since it might affect the dependability of the output. Multiphase flow method VOF calculates liquid-vapor dispersion by volume fraction. Evaporation and condensation rates must be accurately predicted to simulate the phase change process, which affects temperature and flow distribution [12]. Phase change frequency is the rate at which liquids and solids evaporate into vapor. Ignoring phase change or evaporation frequency may restrict the simulation's capacity to predict multiphase system behavior. This may lead to inaccurate outcomes that need time and money to fix. This simulation compares the results of each prototype by changing the evaporation frequency to 0.1, 1, 2, 40, and 160.

RESULTS AND DISCUSSIONS

Post-processing of the simulation will provide the outcomes of the simulation. The results that will be discussed in this section include cold (R717) vapor fraction, temperature difference, and pressure drops.

Comparison Between Prototypes

Referring to Figure 6, each of these three prototypes undergoes a multiphase simulation that considers the boundary conditions that have been set for it. At 303.15K, heat transfer from hot water causes R717 liquid to convert into R717 vapor, so it can be concluded that all prototypes can vaporize the liquid well. This comparison between prototypes uses the default value of evaporation frequency of 0.1.

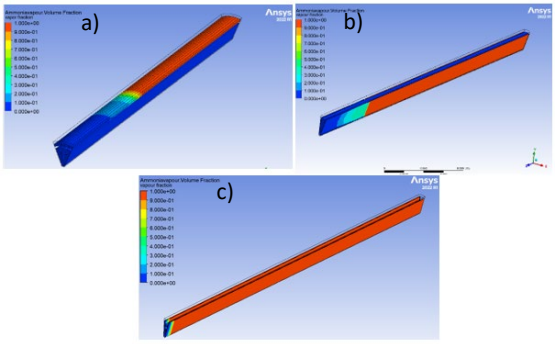

Figure 6: R717 vapor fraction formed for Prototype (a)1, (b) 2 and (c) 3.

Simulation Validation

Validation of simulation models is required to demonstrate the accuracy and dependability of the simulation model. The purpose of simulating with varying evaporation frequencies is to compare the outcomes of each prototype. In this study, the simulation is validated by an experiment conducted in a previous study using the same fluid properties, R717 ammonia, and water [13].

However, there is a significant difference between the heat exchanger's boundary conditions and its design model. The variances in percentage error between CFD simulations and experimental findings will be further discussed. Thus, evaporation frequencies for each prototype are 160, 40, and 1. Due to the large difference in boundary conditions and heat exchanger design between simulation and experiment, few high percentage error values exist. Table 7 shows the lowest percentage error among others. Therefore, performance evaluation based on selected evaporation frequency for each prototype will be further discussed.

Cold Vapor Fraction

Figure 7 depicts the R717 vapor fraction formed along the 0.5m heat exchanger pipe for each prototype based on the 160, 40, and 1 evaporation frequencies, respectively. Overall, it is evident that Prototype 2 has the highest rate of vaporization compared to other prototypes. This is due to the efficiency of the heat exchanger even though some factors might happen to contradict the performance of the heat exchanger such as the wetted area.

Table 7: Comparison between simulation and experiment for each prototype.

PROTOTYPE 1	Evaporation Frequency			160		
		Simulation	ΔT	Experiment	ΔT	Error (%)
	Inlet R717	287.45	12.55	285.55	8.1	54.94
	Outlet R717	300		293.65		
	Inlet water	303.15	2.07	300.15	2.5	17.02
	Outlet water	301.08		297.65		
PROTOTYPE 2	Evaporation Frequency			40		
		Simulation	ΔT	Experiment	ΔT	Error (%)
	Inlet R717	287.45	12.55	285.55	8.1	54.94
	Outlet R717	300		293.65		
	Inlet water	303.15	2.66	300.15	2.5	6.28
	Outlet water	300.49		297.65		
PROTOTYPE 3	Evaporation Frequency			1		
		Simulation	ΔT	Experiment	ΔT	Error (%)
	Inlet R717	287.45	12.55	285.55	8.1	54.94
	Outlet R717	300		293.65		
	Inlet water	303.15	1.54	300.15	2.5	38.52
	Outlet water	301.61		297.65		

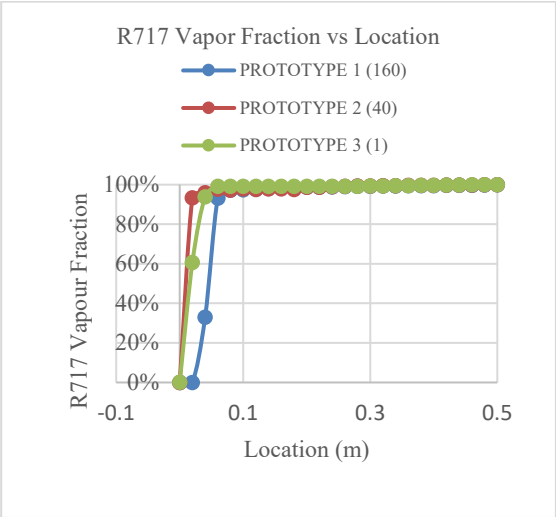

Figure 7: Graph of R717 vapor fraction vs Location

Outlet Temperatures

The temperature of both cold and hot fluids will be evaluated assessing the hat exchanger's effectiveness. Both Figure 8 and Figure 9 depict the cold and hot outlet temperatures, respectively. The outlet cold temperature of all prototypes appears to be the same at 300K, whereas the outlet hot temperature is highest for Prototype 3 at 301.6K, followed by Prototype 1 at 301.1 K. The Prototype 2 hot outlet temperature is known to be the lowest at 300.5K. The effectiveness of the heat exchanger will be further discussed in relation to the temperature.

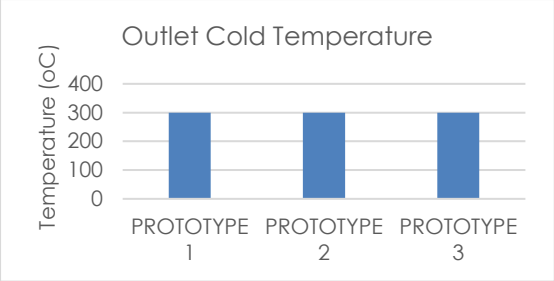

Figure 8: Outlet cold temperatures for each prototype

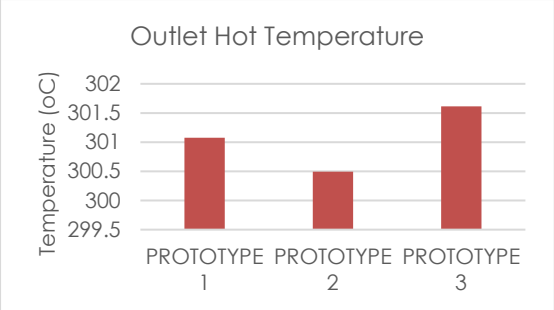

Figure 9: Outlet hot temperatures for each prototype

Cold Vapor Fraction

The performance of the heat exchanger will be evaluated by the effectiveness and the overall heat transfer coefficient where the prototypes show their significant performance due to several factors such as the wetted area and design of the heat exchanger. The net power production per heat transfer area in a single channel is the most crucial factor for comparing the efficiency of different heat exchangers, especially when dealing with variables [14].

Heat Transfer Rate

Calculating the heat transfer rate of a heat exchanger is one method to assess its efficiency. The heat transfer rate of a heat exchanger is used to determine its efficiency. Table 8 shows the overall heat transfer rate based on equations (1) and (2).

$$\dot{Q}_{hot} = \dot{m} C_p \Delta T \quad (1)$$

$$\dot{Q}_{cold} = \dot{m}(h_2 - h_1) \quad (2)$$

Where:
$\dot{Q}$: heat transfer per unit time (kW)
$\dot{m}$: mass flow rate (kg/s)
C_p: specific heat at constant pressure (kJ/kgK)
ΔT: temperature difference
h: enthalpy (kJ/kg)

Table 8: Overall heat transfer rate for each prototype

Prototype	Cold Fluid Heat Transfer Rate, Q (kW)	Hot Fluid Heat Transfer Rate, Q (kW)	Overall Heat Transfer Rate, Q (kW)
Prototype 1	14.2197	19.5111	33.7309
Prototype 2	14.2192	24.9884	39.2076
Prototype 3	14.2191	24.0562	38.2753

Wetted Area

Heat transfer study shows that the wetted area, or fluid contact area affects heat transfer. The wet area for each prototype is considered based on the solid area on which the heat transfer occurs between the hot fluid and the cold fluid. Table 9 portrays the comparison of the wetted area of each prototype:

Table 9: Wetted area for each prototype.

Prototype	Wetted Area (m^2)
Prototype 1	0.0175
Prototype 2	0.0376
Prototype 3	0.0410

Log Mean Temperature Difference (LMTD)

LMTD is the temperature variation used in heat exchanger studies to determine the fundamental heat transfer between two fluids. By comparing the temperature at both ends of the heat exchanger, the LMTD may be utilized as a substitute for the average temperature gradient along the whole heat exchanger which can be seen in Table 10.

$$LMTD = \frac{(T_{in,hot} - T_{out,cold}) - (T_{out,hot} - T_{in,cold})}{ln(T_{in,hot} - T_{out,cold}) - ln(T_{out,hot} - T_{in,cold})} \quad (3)$$

Where:
$T_{in,hot}$: Inlet water temperature (K)
$T_{out,hot}$: Outlet water temperature (K)
$T_{in,cold}$: Inlet R717 temperature (K)
$T_{out,cold}$: Outlet R717 temperature (K)

Table 10: LMTD values for each prototype.

Prototype	LMTD
Prototype 1	7.1527
Prototype 2	6.9628
Prototype 3	7.3263

Overall Heat Transfer Coefficient

The overall heat transfer coefficient describes the efficiency with which heat is conveyed from one fluid to another across an interface. Table 11 shows

the comparison between the prototypes. The overall heat transfer coefficient is calculated by:

$$U = \frac{\dot{Q}}{A \times LMTD} \quad (4)$$

Where:
$\dot{Q}$: heat transfer per unit time (kW)
A: heat transfer area (m2)
$LMTD$: Log Mean Temperature Difference

Table 11: Overall heat transfer coefficient for each prototype

Prototype	Overall Heat Transfer Coefficient, U
Prototype 1	269.4741
Prototype 2	156.4178
Prototype 3	127.4245

Number Transfer Unit

The NTU (Number of Transfer Units) method is widely employed for evaluating heat exchanger performance and estimating heat transfer rates. The comparison value can be seen in Table 12. The NTU method can be calculated by using Cmin which is the product of the mass flow rate and specific heat for constant pressure:

$$\text{NTU} = \frac{UA}{C_{min}} \quad (5)$$

Where:
U: overall heat transfer coefficient
A: heat transfer area (m2)
C_{min}: smallest thermal capacity for single-phase fluid

Table 12: NTU value for each prototype

Prototype	Overall Heat Transfer Coefficient, U
Prototype 1	0.7521
Prototype 2	0.8981
Prototype 3	0.8338

Effectiveness Of Heat Exchanger

For comparison of a variable heat exchanger, the net power output per heat transfer area in a single path is the most important factor if we consider the effectiveness of the heat exchangers [14]. The effectiveness is the measure of the performance of the heat exchanger by using the NTU-method approach which the comparison can be seen in Table 13:

$$\varepsilon = 1 - e^{-NTU} \quad (6)$$

Where:
NTU: number transfer units

Table 13: Effectiveness percentage for each prototype

Prototype	Effectiveness (%)
Prototype 1	52.86
Prototype 2	59.27
Prototype 3	56.56

In theory, the optimum efficiency of a counterflow heat exchanger is 1 or 100%, but in practice, this is rarely achieved. In OTEC applications, where the temperature difference between the hot and cold fluid is relatively small, it is essential to have a heat exchanger with a high level of efficiency to maximize the amount of electricity that can be generated. Based on a previous study [14], [15] which focused on the performance of OTEC heat exchangers, the paper discovered that OTEC implementations can achieve efficacies of at least 50%, and up to 70% under certain conditions.

Differences between LMTD and NTU Methods

LMTD and NTU methods have significant differences when evaluating the performance of a heat exchanger. Based on experimental values of the inlet and outlet temperatures and the fluid flow rates, the LMTD method is beneficial for determining the overall heat transfer coefficient, U. If the inlet temperatures and U are known, however, this method is inconvenient for predicting the outlet temperatures. The effectiveness-NTU method provides a more practical technique for predicting outlet temperatures. Without introducing additional assumptions, this method can be derived from the LMTD method. The effectiveness-NTU and LMTD approaches are therefore equivalent. The ability of the effectiveness-NTU method to predict outflow temperatures without employing a numerical iterative solution of a system of nonlinear equations is one of its advantages.

CONCLUSION

This research aimed to create a model of an effective heat exchanger for Ocean Thermal Energy Conversion (OTEC) applications. The model was subjected to comprehensive computational fluid dynamics (CFD) simulation and the results were extensively discussed using relevant concepts and references. Provided are conclusive suggestions for future implementation and analysis of the heat

exchanger. The simulations included vapor fraction formation, temperature difference, and pressure drop across numerous prototypes, among other aspects. Due to its larger wetted area, Prototype 3 demonstrated the maximum heat transfer rate, but some limitations were identified. However, based on the effectiveness, Prototype 2 seems to be the most efficient among the others. The analysis of temperature difference and pressure drop was essential for determining the effectiveness of a heat exchanger. Overall, the new concept heat exchanger prototypes are promising for OTEC applications and contribute to a greater comprehension of evaporation dynamics for design optimization. Compared to simulations, previous studies involving similar fluids, but distinct heat exchanger designs and conditions revealed a large error of up to 54%. To determine the exact evaporation frequency, it is necessary to conduct precise experimentation with the constructed prototype.

ACKNOWLEDGEMENTS

The authors would like to express their appreciation for the support of the Ministry of Higher Education Malaysia (MoHE) for the funding of this research under the registered program cost center #R.J130000.7851.4L893.

REFERENCES

[1] J. L. Holechek, H. M. E. Geli, M. N. Sawalhah, and R. Valdez, "A Global Assessment: Can Renewable Energy Replace Fossil Fuels by 2050?," *Sustainability (Switzerland)*, vol. 14, no. 8, Apr. 2022, doi: 10.3390/su14084792.

[2] A. Mostafaeipour, A. Bidokhti, M. B. Fakhrzad, A. Sadegheih, and Y. Zare Mehrjerdi, "A new model for the use of renewable electricity to reduce carbon dioxide emissions," *Energy*, vol. 238, Jan. 2022, doi: 10.1016/j.energy.2021.121602.

[3] S. M. Masutani and P. K. Takahashi, "Ocean Thermal Energy Conversion (otec)," *Encyclopedia of Ocean Sciences*, pp. 1993–1999, Jan. 2001, doi: 10.1006/RWOS.2001.0031.

[4] L. Aresti, P. Christodoulides, C. Michailides, and T. Onoufriou, "Reviewing the energy, environment, and economy prospects of Ocean Thermal Energy Conversion (OTEC) systems," *Sustainable Energy Technologies and Assessments*, vol. 60, p. 103459, Dec. 2023, doi: 10.1016/J.SETA.2023.103459.

[5] K. Fontaine, T. Yasunaga, and Y. Ikegami, "OTEC maximum net power output using carnot cycle and application to simplify heat exchanger selection," *Entropy*, vol. 21, no. 12, Dec. 2019, doi: 10.3390/e21121143.

[6] R. K. Shah and D. P. Sekulic, "FUNDAMENTALS OF HEAT EXCHANGER DESIGN," 2003.

[7] A. Kasaeian, A. Shamaeizadeh, and B. Jamjoo, "Combinations of Rankine with ejector refrigeration cycles: Recent progresses and outlook," *Appl Therm Eng*, vol. 211, p. 118382, Jul. 2022, doi: 10.1016/J.APPLTHERMALENG.2022.118382.

[8] T. T N *et al.*, "Leveraging artificial neural networks approach for thermal conductivity evaluation in porous rectangular wetted fins filled with ternary hybrid nanofluid," *J Radiat Res Appl Sci*, vol. 17, no. 4, p. 101125, Dec. 2024, doi: 10.1016/J.JRRAS.2024.101125.

[9] N. Samsuri, N. Sazali, A. S. Jamaludin, and M. N. M. Razali, "Performance of Ocean Thermal Energy Conversion Closed Rankine Cycle Using Different Working Fluids," in *IOP Conference Series: Materials Science and Engineering*, IOP Publishing Ltd, Feb. 2021. doi: 10.1088/1757-899X/1062/1/012040.

[10] A. Katz and V. Sankaran, "Mesh quality effects on the accuracy of CFD solutions on unstructured meshes," *J Comput Phys*, vol. 230, no. 20, pp. 7670–7686, Aug. 2011, doi: 10.1016/J.JCP.2011.06.023.

[11] S. Alfarawi, A. El-Sawi, and H. Omar, "Exploring Discontinuous Meshing for CFD Modelling of Counter Flow Heat Exchanger," *Journal of Advanced Research in Numerical Heat Transfer*, vol. 5, no. 1, pp. 26–34, 2021, [Online]. Available: https://www.scopus.com/inward/record.uri?eid=2-s2.0-85122881534&partnerID=40&md5=01fd121405f819333f2c3f50ce24560c

[12] Z. Tan, Z. Cao, W. Chu, and Q. Wang, "Prediction accuracy improvement on evaporation-condensation process via a temperature deviation based dynamic correction model," 2023. [Online]. Available: https://ssrn.com/abstract=4415020

[13] J. Castaing-Lasvignottes, A. Dijoux, F. Sinama, B. Clauzade, O. Marc Marc, and O. Marc, "A presentation of the ocean thermal energy conversion prototype in La Reunion," 2017. [Online]. Available: https://hal.science/hal-02999786v1

[14] T. Yasunaga, T. Noguchi, T. Morisaki, and Y. Ikegami, "Basic heat exchanger performance evaluation method on OTEC," *J Mar Sci Eng*, vol. 6, no. 2, Apr. 2018, doi: 10.3390/jmse6020032.

[15] T. Yasunaga, K. Fontaine, T. Morisaki, and Y. Ikegami, "Performance Evaluation of Heat Exchangers for Application to Ocean Thermal Energy Conversion System," 2017.